Experimental Verification of Driving Force Controller Using High-Power Racing Electric Vehicle

Hiroyuki Fuse* Student Member, Hiroshi Fujimoto* Senior Member
Kenta Yasuda** Non-member, Michita Yanagita** Non-member
Yutaka Awazuhara** Non-member, Seiji Yamamoto** Non-member
Nobuhiro Tajima** Non-member, Yasuhiro Sakoh** Non-member

Nowadays, motorsport has been in a transition of racing vehicle towards electrification. For further development of future electric motorsport, this study pursues ultimate maneuverability of an independent-four-wheel-drive electric vehicle (EV). The group of the authors has developed a driving force controller (DFC) with slip ratio control, which can be used for effective traction control of tire. However, all the experimental verification related to the DFC were only conducted using low-power EV on slippery road. The purpose of this paper is to confirm the effectiveness of the DFC using high-power racing EV on dry road. All-out acceleration without control, with manual pedal control by a professional driver, and with the slip ratio control are compared. The experimental results suggest that the DFC can accelerate the EV as efficient as professional driver, promising enough to adopt it for real high-power racing EVs.

Keywords: electric vehicle, maneuverability, vehicle dynamics, slip ratio control, driving force controller

1. Introduction

Nowadays, electric vehicle (EV) has been a decent candidate for solving environmental problems such as global warming, atmospheric pollution, and shortage of natural resources. However, EV has relatively short driving range because of the capacity of the limited energy storage and a lot of research has been done in order to extend the short driving range [(1) (2)]. While EV shows its environmental potential, it also has several advantages in controllability and maneuverability since it is equipped with electric motors as follows [(3)].

(1) Fast torque control response within several milliseconds
(2) Torque and driving force can be easily estimated
(3) Capability of acceleration and deceleration
(4) Capability of independent-four-wheel-drive (4WD) system

Exploiting these advantages, a lot of traction control and motion stabilization methods have been proposed [(4) (5)].

The group of the authors has proposed a driving force controller (DFC) [(4)], which controls driving force references while maintaining tire's traction that is realized by limiting slip ratio within certain range. By applying the DFC to each wheel, the traction of all wheels can be guaranteed.

The group of the authors has made extensive research on DFC, such as driving force distribution methods [(6) (7)] based on the control of slip ratio, and extensions for cornering by considering sideslip angle [(8) (9)].

All the experimental verifications of the previous work related to DFC were conducted using an EV with directly-driven in-wheel-motor (DD-IWM) on a slippery road. The experimental condition was not common due to mainly two reasons as follows. First, although DD-IWM has advantages in controllability thanks to the lack of reduction gears which is the cause of the lower bandwidth, it tends to be larger than IWM with reduction gears (RG-IWM) and more expensive compared to RG-IWM and on-boarded motor. Second, the experimental vehicle of the previous research has only enough power output to make tire skid on slippery road. Therefore, there was no experimental verification on high grip road using high-power-output EV so far.

In order to verify the effectiveness of the DFC on wider range of conditions and situations, this paper conducts an experimental verification of the DFC on dry road using a real high-power racing EV. The experimental result shows the effectiveness of the DFC on acceleration from standstill compared to that of without control and manual throttle control by professional driver. The rest of this paper is as follows. First, vehicle model of an independent-4WD EV is defined. Next, the detail of the DFC is explained. Third, the experimental vehicle and its specification is described. Then, simulations and an experiment of acceleration of the experimental vehicle is shown.

2. Vehicle Model

2.1 Vehicle model In this paper, we consider a vehicle that is capable of independent-4WD. Fig.1 shows an illustration of the vehicle model.

It is assumed that steering angle of left and right side are equal. Load transfer due to acceleration is taken into account. In the figure, a_x, a_y, V, β, γ, α_{ij} are longitudinal, lateral acceleration, vehicle velocity, vehicle's sideslip angle, yaw rate,

* The University of Toyko
5–1–5, Kashiwanowa, Kashiwa-shi, Chiba, Japan 277–8561
** TAJIMA EV Corporation
3–1–15, Sakashita, Itabashi, Tokyo, Japan 174–0043

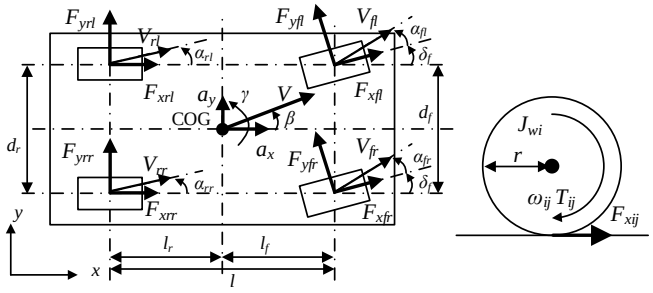

Fig. 1 Vehicle model.

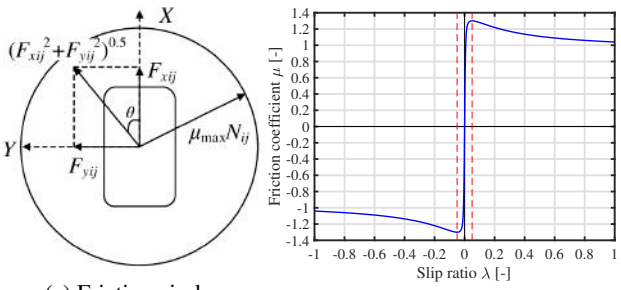

(a) Friction circle.

(b) λ–μ curve ($\alpha = 0$).

Fig. 2 Tire force model. Friction circle dictates the limit of tire force and the trade-off between longitudinal and lateral direction. There is an optimal slip ratio λ_{p0} where friction coefficient takes its peak. The λ–μ curve is the approximated characteristic of the tire of the experimental vehicle.

and sideslip angle of each wheel. The subscription of i will be f or r, indicating front or rear wheel, and j will be l or r, indicating left or right respectively. Equation of rotation of wheel is given by

$$J_{\omega_i}\dot{\omega}_{ij} = T_{ij} - rF_{xij}, \cdots\cdots (1)$$

where $J_{\omega_{ij}}$, ω_{ij}, T_{ij}, r, and F_{xij} are wheel's inertia, angular velocity, torque, radius of tire, and tire longitudinal force, respectively. As for vehicle, equations of vehicle dynamics are given by

$$\begin{aligned} Ma_x &= (F_{xfl} + F_{xfr})\cos\delta_f - (F_{yfl} + F_{yfr})\sin\delta_f \\ &\quad + (F_{xrl} + F_{xrr}) \cdots\cdots (2) \\ Ma_y &= (F_{xfl} + F_{xfr})\sin\delta_f + (F_{yfl} + F_{yfr})\cos\delta_f \\ &\quad + F_{yrl} + F_{yrr}) \cdots\cdots (3) \\ I\dot{\gamma} &= \frac{d_f}{2}(-F_{xfl} + F_{xfr})\cos\delta_f + l_f(F_{xfl} + F_{xfr})\sin\delta_f \\ &\quad + l_f(F_{yfl} + F_{yfr})\cos\delta_f + \frac{d_f}{2}(F_{yfl} - F_{yfr})\sin\delta_f \\ &\quad + \frac{d_r}{2}(-F_{xrl} + F_{xrr}) - l_r(F_{yrl} + F_{yrr}), \cdots\cdots (4) \end{aligned}$$

where M, F_{yij}, δ_i, γ, I, l_i, and d_i are vehicle mass, tire lateral force, steering angle, yaw rate, vehicle inertia, distance between COG and axle of wheel, and tread. For the simplicity, we do not consider suspension dynamics or aerodynamics for simulations.

2.2 Tire Model To get a better understanding of the DFC. this section describes basic properties of tire force. It is important to get the exact information of tire forces F_{xij} and F_{yij} so that we can obtain the maneuver of vehicle using the equations of vehicle dynamics above. However, it is not easy to obtain these forces since the generation of tire forces involves complicated friction phenomena between road and tire. Therefore, a lot of tire models have been proposed to emulate the generation of tire forces with different purpose and focus such as brush model [10], Magic Formula [11], and λ-Method tire model.

2.2.1 Friction Circle and Tire Workload Assuming maximum friction coefficient $\mu_{\max}$, resultant force F_{ij}, longitudinal force F_{xij}, lateral force F_{yij}, normal reaction force N_{ij}, and the direction of resultant force θ, the following equations have to be satisfied.

$$F_{ij} = \sqrt{F_{xij}^2 + F_{yij}^2} \le \mu_{\max}N_{ij} \cdots\cdots (5)$$

$$\theta = \tan^{-1}\frac{F_{yij}}{F_{xij}} \cdots\cdots (6)$$

This concept is called a friction circle shown in Fig.2a, indicating tire force has its limit determined by the condition of road and tire, and normal reaction force acting on tire. Tire workload η_{ij} is defined by

$$\eta_{ij} = \frac{\sqrt{F_{xij}^2 + F_{yij}^2}}{\mu_{\max}N_{ij}} \le 1. \cdots\cdots (7)$$

If tire workload is close to 1, so is tire force close to its limit.

2.2.2 Generation of Tire Force In general, longitudinal and lateral force are generated by slip ratio and sideslip angle respectively. In this paper, slip ratio λ_{ij} is defined by

$$\lambda_{ij} = \frac{V_{\omega_{ij}} - V_{ij}}{\max(V_{\omega_{ij}}, V_{ij})} \cdots\cdots (8)$$

where $V_{\omega_{ij}} = r\omega_{ij}$. The relation between slip ratio λ and friction coefficient of road μ is nonlinear as shown in Fig.2b. To emulate this, Magic formula [11] is widely used given by

$$\mu(\lambda) = \sin\left(C\tan^{-1}B\left[(1-E)\lambda + \frac{E}{B}\tan^{-1}B\lambda\right]\right). \cdots (9)$$

The friction coefficient takes its maximum value $\mu_{\max}$ at a certain slip ratio called optimal slip ratio λ_{p0} when $\alpha = 0$.

2.3 Experimental Vehicle In this paper, we use a high-power racing EV "E-runner 2016" shown in Fig.4 for experimental verification. The EV is equipped with four of on-boarded motor for each wheel and capable of independent 4WD control. This EV ran at Pikes Peak International Hill Climb Championship in 2016 and won the third place in the EV division. For the experiment, a professional rally driver Yutaka Awazuhara, nine-time Japanese Rally Championship winner, took the wheel for safety and the experimental comparison between manual throttle control against the DFC.

Table.1 and Table.2 show the specification of the experimental vehicle.

3. Driving Force Controller

In this section, a DFC [6] is explained.

3.1 Block Diagram and Structure The block diagram of the DFC is shown in Fig.3. The DFC generally assumes that reference driving force $F_{xij}{}^*$ is generated as human driver presses accelerator pedal manually. The feedforward loop mainly works quickly when EV is on dry road

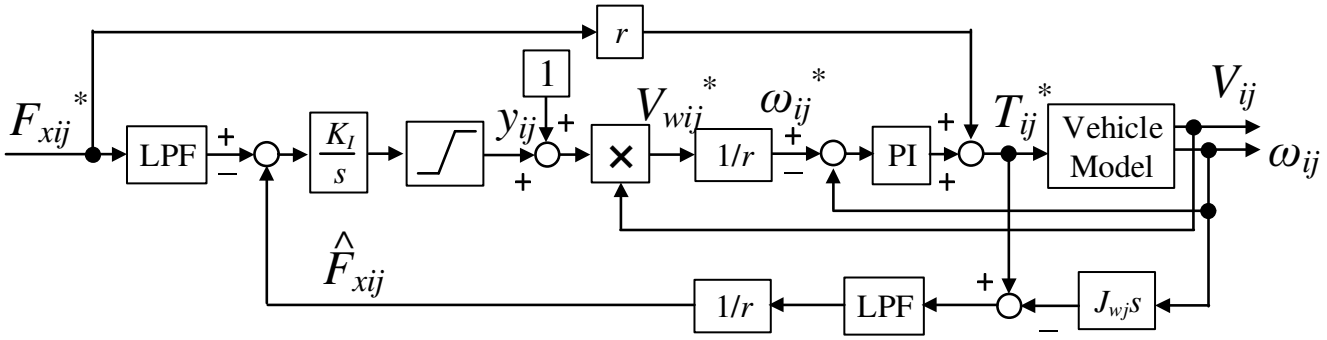

Fig. 3 Driving Force Controller (DFC). Feedforward loop secures fast response, and feedback loop adjusts slight error. The inner slip ratio limiter works as traction control.

Fig. 4 E-runner 2016, high-power racing EV for the experimental verification.

Tab. 1: Vehicle specification and performance.

Vehicle mass M	1605 kg
Wheelbase l	2.7 m
Distance from center gravity to front and rear axle l_f, l_r	l_f:1.31 m l_r:1.39 m
Gravity height h_g	0.33 m
Tread d_f, d_r	1.62, 1.68 m
Equivalent front and rear wheel inertia $J_{\omega f}$, $J_{\omega r}$	$J_{\omega f}$ = 0.95 kg·m^2 $J_{\omega r}$ = 0.95 kg·m^2
Wheel radius r	0.35 m
Optimal slip ratio λ_{p0}	0.04-0.05
Drivetrain	Chain-driven System
Gear ratio	6.11
0-100 km/h acceleration	2.2 s
Top speed	270 km/h

Tab. 2: Specification of electric motors.

	Front	Rear
Manufacturer	Rimac Automobili	
Rated torque	250 Nm	300 Nm
Maximum torque	330 Nm	424 Nm
Rated power	160 kW	193 kW
Maximum power	319 kW	327 kW
Maximum speed	10600 rpm	10600 rpm

where enough driving force can be generated. The outer feedback loop determines how much slip ratio reference is generated by comparing $F_{xij}{}^*$ and the estimated longitudinal force $\hat{F}_{xij}$ which is obtained by a driving force observer (DFO). For example, if sufficient longitudinal force is not generated, reference slip ratio increases so that tire generates more longitudinal force as desired. The inner feedback loop is a slip ratio/wheel velocity loop that controls slip ratio. The definition of slip ratio has two cases on both acceleration and deceleration as seen in (8). For smoother control, new control input y_{ij} is defined as

$$y_{ij} = \frac{V_{\omega_{ij}} - V_{ij}}{V_{ij}} \cdots\cdots (10)$$

This is the same definition as that of slip ratio for deceleration. The relationship between y_{ij} and λ_{ij} for acceleration is calculated as

$$y_{ij} = \frac{\lambda_{ij}}{1 - \lambda_{ij}} \cdots\cdots (11)$$

y_{ij} approximately equals to λ_{ij} when $|\lambda_{ij}| << 1$ and they are always one to one correspondence.

3.2 Slip Ratio Limiter and Traction Control Magic formula tire model suggests that longitudinal force F_x rather decreases if slip ratio λ exceeds optimal slip ratio λ_{p0}. Therefore, if $F_{xij}{}^*$ becomes larger than what tire and road can produce (i.e., in case of slippery road or EV has too much power), increase of slip ratio reference causes tire slips and no more longitudinal force is generated. This situation should be avoided for safer drive. To achieve this, upper and lower limit of slip ratio reference y_{ijmax} and y_{ijmin} for the integrator of the DFC are added. With this saturation, traction can be retained by keeping the slip ratio within the range where μ is monotonic function of λ (see Fig.2b).

4. Experimental Verification

4.1 Experimental setup Experimental verification of the DFC was conducted using the experimental vehicle on dry road. All-out acceleration was attempted with three situations; full-throttle without control, manual pedal control by professional driver, and slip ratio control with the reference λ^* = 0.02, 0.04, 0.06, and 0.10 as shown in Fig.5. Table.3 shows the experimental condition. Fig.6 shows a picture of experimental field during the experiment of all-out acceleration without control.

For safety reason, only front wheels were driven. Motor torque was limited by 280 Nm (270 Nm in case of manual control). PI gain K_P, K_I of the inner slip ratio-wheel velocity controller were determined using pole allocation as follows. The nominal wheel inertia $J_{\omega n}$ was set with a nominal slip

Tab. 3: Experimental condition.

Driving wheel	Front wheels (so called "FF")
Torque limit	280 (manual: 270) Nm
PI controller	$\lambda_n = 0.1$, $\omega_n = 2$ rad/s
Optimal slip ratio λ_{p0}	0.04-0.05

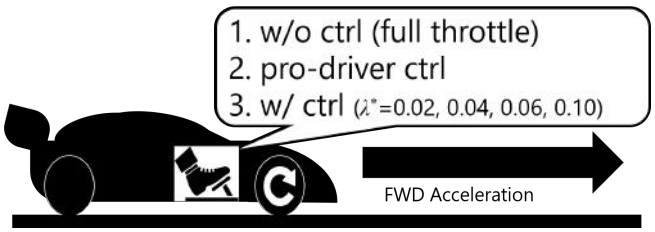

Fig. 5 Illustration of the experiment.

ratio $\lambda_n = 0.1$. The pole of the controller ω_c was set to be 2 rad/s. To be the comparison of each case fair, tire temperature was maintained to be cool (i.e., without warming up).

$$K_P = 2J_{\omega n}\omega_c \quad \cdots\cdots (12)$$

$$K_I = J_{\omega n}\omega_c^2 \quad \cdots\cdots (13)$$

$$J_{\omega n} = J_{\omega f} + \frac{r^2 M}{2}(1-\lambda_n) \quad \cdots\cdots (14)$$

Tab. 4: Comparison of average acceleration from $V = 10$ m/s to $V = 15$ m/s. Slip ratio control with $\lambda^* = 0.10$ demonstrates the fastest acceleration.

Ctrl method	Average a_x m/s^2
w/o ctrl (full throttle)	3.32
Pro-driver ctrl	3.81
w/ ctrl $\lambda^* = 0.02$	3.18
w/ ctrl $\lambda^* = 0.04$	3.73
w/ ctrl $\lambda^* = 0.06$	3.75
w/ ctrl $\lambda^* = 0.10$	3.88

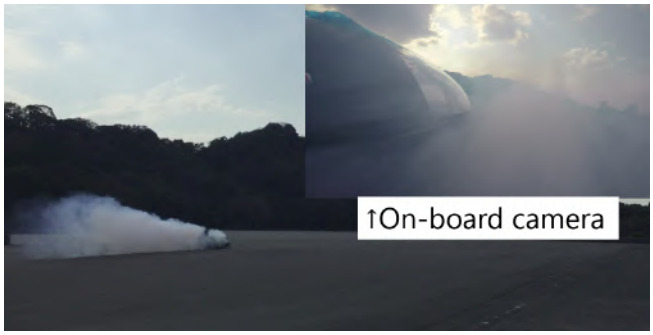

Fig. 6 Full-throttle acceleration without control. Wheels slip so much that huge amount of white smoke covers almost entire vehicle.

4.2 Results Fig.7, Fig.8, Fig.9, Fig.10, Fig.11, and Fig.12 show experimental results of all-out acceleration with front two wheels on dry road in case of full-throttle without control, manual pedal control by professional driver, and slip ratio control with the reference $\lambda^* = 0.02$, 0.04, 0.06 and 0.10, respectively.

In the figures of motor torque T_m, Green dashed line indicates the torque limit. Black dashed line with the caption of either "Acc" or "Ctrl" are also shown. Acc means the level of throttle in the unit of %. When Ctrl is nonzero, slip ratio control is being activated.

In case of all-out acceleration without control (see Fig.7), Torque input becomes maximized quickly, with the increase of slip ratio up to 0.8 with wheel velocity of 70 m/s. Around 1 s, safety system activates as input torque exceeds its limit value and starts to decrease. Longitudinal acceleration a_x only reaches around 3 m/s^2. During the acceleration, huge while smoke occurred as seen in Fig.6. Such the smoke was only seen in this case.

With manual pedal control by professional driver (see Fig.8), torque input is adjusted and slip ratio is suppressed up to 0.6 with wheel velocity of 20 m/s, much less than without control. Thanks to the manual torque control, longitudinal acceleration a_x reaches around 4 m/s^2. As vehicle velocity V reaches to 20 m/s, slip ratio maintains low value even though torque input is maximum. This is because of the increase of downforce (i.e., traction) and unmeasurable resistive force (such as rolling resistance, gear friction, and air drag).

In case of acceleration of slip ratio control with $\lambda^* = 0.02$ (see Fig.9), slip ratio is drastically suppressed. Torque input rarely reaches to its limit, which is due to the lower slip ratio reference than the optimal slip ratio $\lambda_{p0} = 0.04$. Longitudinal acceleration a_x is slightly smaller than 4 m/s^2. This means the reference value $\lambda^* = 0.02$ can be useful for close-to-limit acceleration with saving tire's lifetime.

Acceleration of slip ratio control with $\lambda^* = 0.04$, 0.06, and 0.10 demonstrate basically the same tendency. When vehicle velocity V is lower than 20 m/s, torque input is limited to be less than the maximum value 280 Nm in order to maintain desired slip ratio. During this period, longitudinal acceleration a_x is slightly lower than 4 m/s^2. As vehicle velocity V exceeds 20 m/s, torque input becomes maximized and slip ratio decreases to 0.01. The reason why the three cases show similar acceleration is that the tire of the experimental vehicle has its optimal slip ratio λ_{p0} around 0.04 - 0.05 and the friction coefficient does not decrease much even slip ratio becomes 0.10 (see the approximated λ–μ curve of the tire in Fig.2b).

It is observed that left and right slip ratio alternately change (Fig.9, Fig.10, Fig.11, and Fig.12). The cause is the fluctuation of road condition (such as bump, different pavement, etc.), low gain of the slip ratio controller due to the limitation of the chain-driven system of the experimental vehicle. When left and right slip ratio alternately change, lateral acceleration a_y changes at the same time. This heavily implies that load transfer between left and right wheels occurred rapidly.

Table.4 shows comparison of average acceleration from vehicle velocity $V = 10$ m/s to $V = 15$ m/s when wheel tends to slip without torque control. The manual pedal control by professional driver has better acceleration than without control. Slip ratio control with $\lambda^* = 0.04$ and 0.06 has slightly lower but pretty close average acceleration compared to the manual pedal control. Not only that, slip ratio control with $\lambda^* = 0.10$ has better result than the manual pedal control. The reason that slip ratio control with $\lambda^* = 0.10$ demonstrates the best result is that it always maintains slip ratio larger than the optimal slip ratio λ_{p0} of the experimental vehicle. Therefore,

the DFC with slip ratio control has great potential that can be even used for high-power racing EV, with close or better performance of acceleration.

The experiment was only conducted on acceleration, but the DFC will perform great deceleration as well since there is no concern of the change of performance which would occur in case of mechanical brake due to the heat. Further experimental verification on deceleration, and other situations involving cornering will be future work.

5. Conclusion

Towards the development of future electric motorsport, this study pursues ultimate maneuverability of an independent-four-wheel-drive electric vehicle. As one step ahead, this paper conducted experimental verification of the driving force controller with slip ratio control using high-power racing EV on dry road. All-out acceleration without control, with manual pedal control by a professional driver, and with the slip ratio control were compared. The experimental results showed that the DFC can accelerate the EV as efficient as professional driver, with the average acceleration from vehicle velocity of 10 m/s to 15 m/s by manual pedal control and the slip ratio control with reference of 0.1 were 3.81 m/s^2 and 3.88 m/s^2, respectively, which is promising enough to adopt it for real high-power racing EVs. Currently, further experimental verifications of EV's motion control methods developed by the authors are underway.

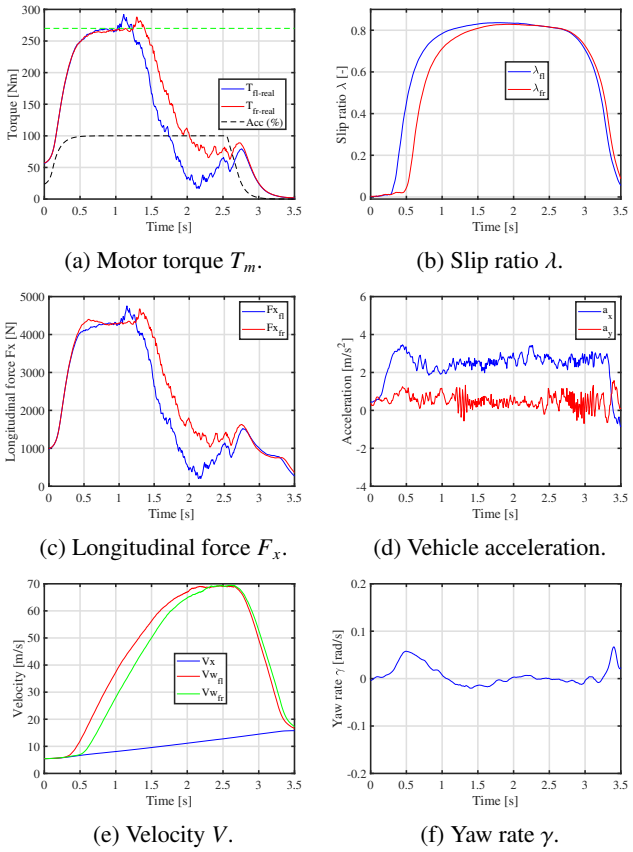

(a) Motor torque T_m. (b) Slip ratio λ.

(c) Longitudinal force F_x. (d) Vehicle acceleration.

(e) Velocity V. (f) Yaw rate γ.

Fig. 7 All-out acceleration without control (full-throttle). Slip ratio went up to 0.8, with the wheel velocity of nearly 70 m/s.

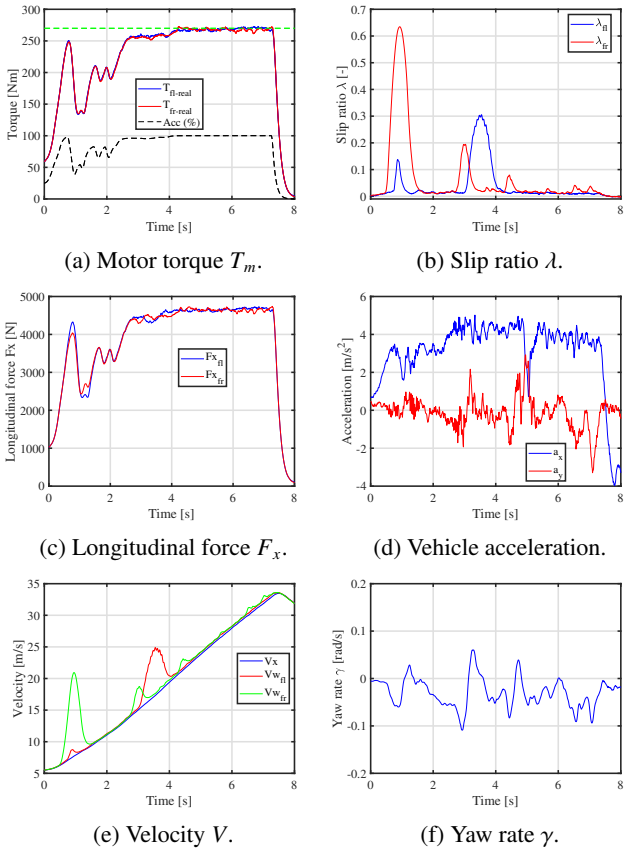

(a) Motor torque T_m. (b) Slip ratio λ.

(c) Longitudinal force F_x. (d) Vehicle acceleration.

(e) Velocity V. (f) Yaw rate γ.

Fig. 8 All-out acceleration with throttle control by a professional driver.

References

(1) Y. Ikezawa, et. al., "Range Extension Autonomous Driving for Electric Vehicles Based on Optimal Velocity Trajectory Generation and Front-Rear Driving-Braking Force Distribution," IEEJ J. Industry Applications, vol. 5, no. 3, pp. 228–235, 2016.

(2) G. Lovison, et. al.,"Secondary-side-only Control for High Efficiency and Desired Power with Two Converters in Wireless Power Transfer Systems,"IEEJ J. Industry Applications, vol. 6, no. 6, pp. 473–481, 2017.

(3) Y. Hori, "Future vehicle driven by electricity and control research on four-wheel-motored "UOT electric march II"", IEEE Trans. Industrial Electronics, 51, 5, pp. 954-962 (2004).

(4) M. Yoshimura and H. Fujimoto, "Driving torque control method for electric vehicle with in-wheel motors", IEEJ Transactions on Industry Applications, Vol. 131, No. 5, pp.1-8 (2010) (in Japanese).

(5) M. Kamachi, and K. Walters: "A Research of Direct Yaw- Moment Control on Slippery Road for In-Wheel Motor Vehicle", The 22nd International Battery, Hybrid and Fuel Cell Electric Vehicle Symposium and Exposition, Yokohama, Japan, pp. 2122-2133 (2006).

(6) K. Maeda, H. Fujimoto, and Y. Hori: "Four-wheel Driving force Distribution Method for Instantaneous or Split Slippery Roads for Electric Vehicle with in-wheel motors", 12th IEEE International Workshop on Advanced Motion Control, pp. 1-6. (2012).

(7) N.Shimoya, H.Fujimoto, "Fundamental Study of Driving Force Distribution Method for Minimization of Maximum Slip Ratio for Electric Vehicles with In-wheel Motors", International Electric Vehicle Technology Conference (EVTeC), 2016.

(8) K. Maeda, H. Fujimoto, Y. Hori, "Driving Force Control of Electric Vehicle Based on Optimal Slip Ratio Estimation Using brush model", JIASC, Vol. IV, pp. 137-140, 2012.

(9) H. Fuse, H. Fujimoto. "Fundamental Study on Driving Force Control Method for Independent-Four-Wheel-Drive Electric Vehicle Considering Tire Slip Angle", IEEE conference IECON2018, 2018.

(10) O. Nishihara, et-al, "Estimation of Road Friction Coefficient Based on the Brush Model", Transactions of the Japan Society of Mechanical Engineers Series C 75(753), 1516-1524, 2009. (in Japanese).

(11) H. B. Pacejka and E. Bakker, "The Magic Formula Tyre Model," Vehicle System Dynamics: International Journal of Vehicle Mechanics and Mobility, Vol. 21, No. 1, pp. 1-18 (1992).

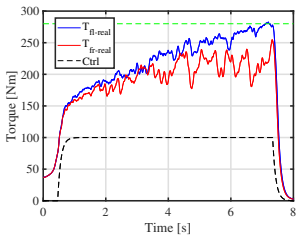

(a) Motor torque T_m.

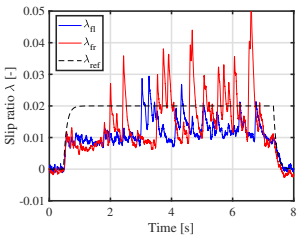

(b) Slip ratio λ.

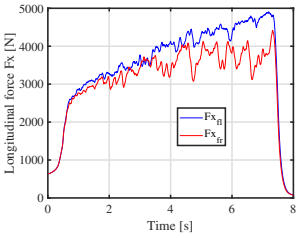

(c) Longitudinal force F_x.

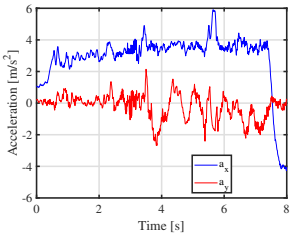

(d) Vehicle acceleration.

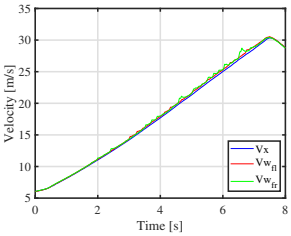

(e) Velocity V.

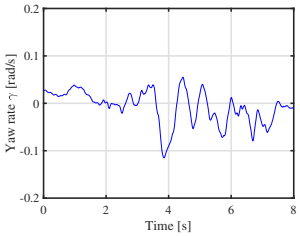

(f) Yaw rate γ.

Fig. 9 All-out acceleration with slip ratio control (λ^* = 0.02).

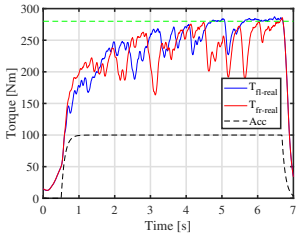

(a) Motor torque T_m.

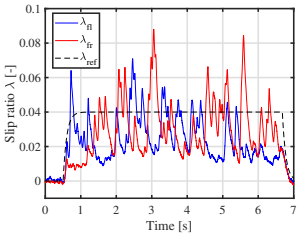

(b) Slip ratio λ.

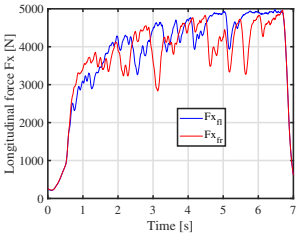

(c) Longitudinal force F_x.

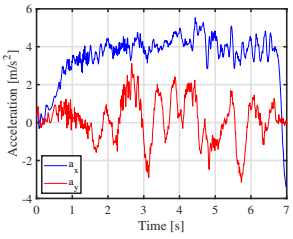

(d) Vehicle acceleration.

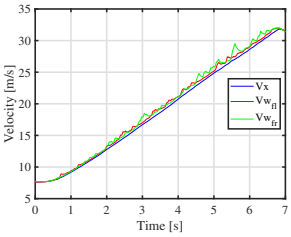

(e) Velocity V.

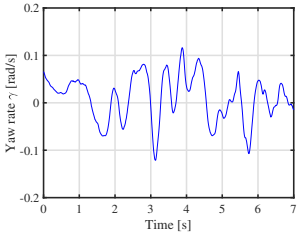

(f) Yaw rate γ.

Fig. 10 All-out acceleration with slip ratio control (λ^* = 0.04).

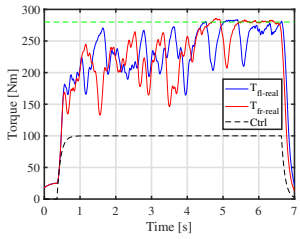

(a) Motor torque T_m.

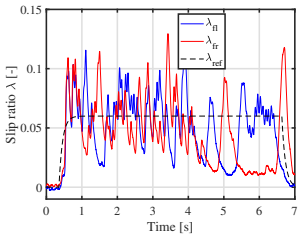

(b) Slip ratio λ.

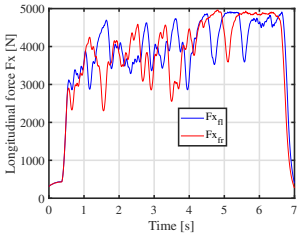

(c) Longitudinal force F_x.

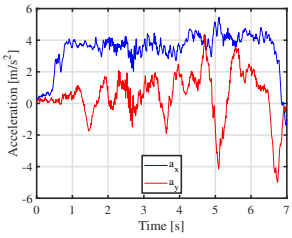

(d) Vehicle acceleration.

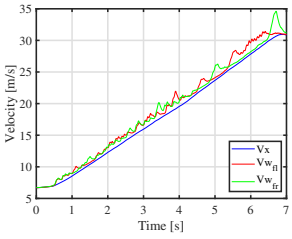

(e) Velocity V.

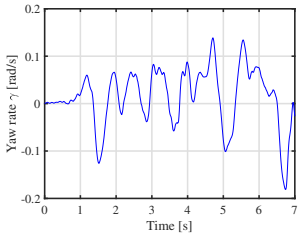

(f) Yaw rate γ.

Fig. 11 All-out acceleration with slip ratio control (λ^* = 0.06).

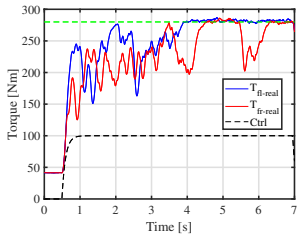

(a) Motor torque T_m.

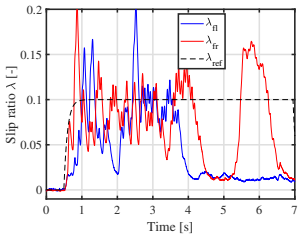

(b) Slip ratio λ.

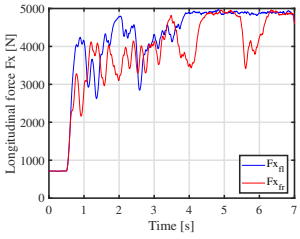

(c) Longitudinal force F_x.

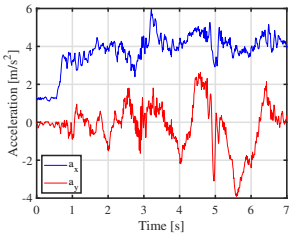

(d) Vehicle acceleration.

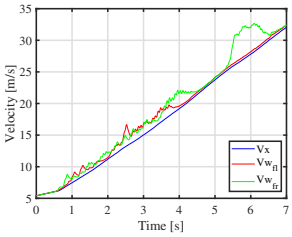

(e) Velocity V.

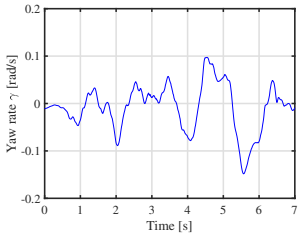

(f) Yaw rate γ.

Fig. 12 All-out acceleration with slip ratio control (λ^* = 0.10).